DOI: 10.1478/AAPP.961A3

AAPP | Atti della Accademia Peloritana dei Pericolanti
Classe di Scienze Fisiche, Matematiche e Naturali
ISSN 1825-1242

Vol. 96, No. 1, A3 (2018)

PATIENT DOSE IN IMAGE GUIDED RADIOTHERAPY: MONTE CARLO STUDY OF THE CBCT DOSE CONTRIBUTION

SALVATORE LEOTTA,[a] ERNESTO AMATO,[bc*] NICOLA SETTINERI,[d]
EMILIA BASILE,[d] ANTONIO ITALIANO,[c] LUCREZIA AUDITORE,[ce]
ANNA SANTACATERINA,[d] AND STEFANO PERGOLIZZI [be]

ABSTRACT. Image Guided RadioTherapy (IGRT) is a technique whose diffusion is growing thanks to the well-recognized gain in accuracy of dose delivery. However, multiple Cone Beam Computed Tomography (CBCT) scans add dose to patients, and its contribution has to be assessed and minimized. Aim of our work was to evaluate, through Monte Carlo simulations, organ doses in IGRT due to CBCT and therapeutic MV irradiation in head-neck, thorax and pelvis districts. We developed a Monte Carlo simulation in GAMOS (Geant4-based Architecture for Medicine-Oriented Simulations), reproducing an Elekta Synergy medical linac operating at 6 and 10 MV photon energy, and we set up a scalable anthropomorphic model. After a validation by comparison with the experimental quality indexes, we evaluated the average doses to all organs and tissues belonging to the model for the three cases of irradiated district. Scattered radiation in therapy is larger than that diffused by CBCT by one to two orders of magnitude.

1. Introduction

With the development of highly conformal treatment techniques, such as Intensity Modulated Radiation Therapy (IMRT) as well as 3D Conformal Radiotherapy (3D-CRT), the quest for advanced imaging modalities allowing a precise localization of target and organs at risk is increasing. Thanks to recent technological developments, the use of Cone Beam Computed Tomography (CBCT) is increasing in radiation therapy departments as a tool for verifying the correct positioning of the patient: this technique is called Image Guided RadioTherapy (IGRT). As well known, an accurate patient positioning is crucial to achieve the desired results in radiotherapy (RT) treatments. Any displacement of the target region during the course of irradiation leads to larger inhomogeneity of dose deposition, so that undesirable hot or cold dose spots can occur in tumour and in healthy tissue.

CBCT allows radiation oncologists to correct variations in target position before treatment and hence to check whether the tumour region is properly enclosed inside the PTV during treatment (Moore *et al.* 2006). The increasing use of CBCT in RT has led researchers to explore in detail the dose delivery to patients due to this particular imaging technique. It

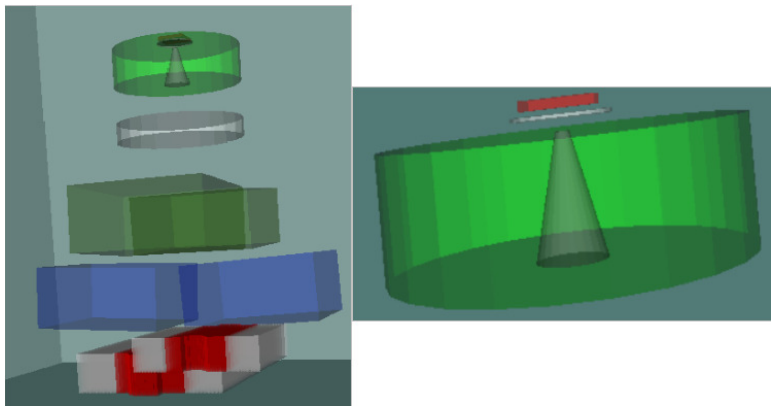

FIGURE 1. on the left, the main components of the head of a medical linac Elekta Synergy: from the top, electrons impact on the tungsten target, leading to the production of bremsstrahlung photons; the flattening filter; circular primary collimator; monitor chambers; two pairs of jaws for secondary collimation; MLC system (central leafs in red). On the right the first three elements are illustrated in detail. z-axis is along beam propagation, top-bottom.

is to be expected that the daily imaging with CBCT delivers a significant dose to patient and therefore an accurate dosimetric characterization of CBCT is very important (Srnivasan *et al.* 2014).

Different studies investigated the dose that CBCT delivers to different organs, reporting that the daily use of CBCT carries a considerable additional dose, leading to an increased risk of secondary tumours (Kan *et al.* 2008). Therefore, in order to prevent the damaging effects of these additional doses, it is essential to quantify them through physical measurements and dedicated Monte Carlo simulations.

The present work was aimed to quantify the doses received by the most important organs during CBCT scan and compare them with the doses received by the same patient during therapies with MV beams. For this purpose, we used GAMOS (Geant4-based Architecture for Medicine-Oriented Simulations) (Arce *et al.* 2012), an application of Geant4 (GEometry ANd Tracking) (Agostinelli *et al.* 2003), through which we carried out a detailed simulation of patients, medical linear accelerator, cone beam computed tomography, thermoluminescence dosimeter and hospital bunker. Our simulation was first validated by comparing the simulated percentage depth doses (PDDs) and the transverse dose profile (X and Y) in a water phantom with those obtained experimentally.

2. Materials and methods

2.1. Monte Carlo simulation. We developed a Monte Carlo simulation using GAMOS (Arce *et al.* 2012), a simulation toolkit provided by Geant4, originally developed for high energy physics and currently applied also in the field of medical radiation physics (Amato *et al.* 2011, 2012, 2013a,b). We reproduced the whole radiotherapy set-up consisting of a medical linear accelerator (LINAC Elekta Synergy), operating at two photon energies (6

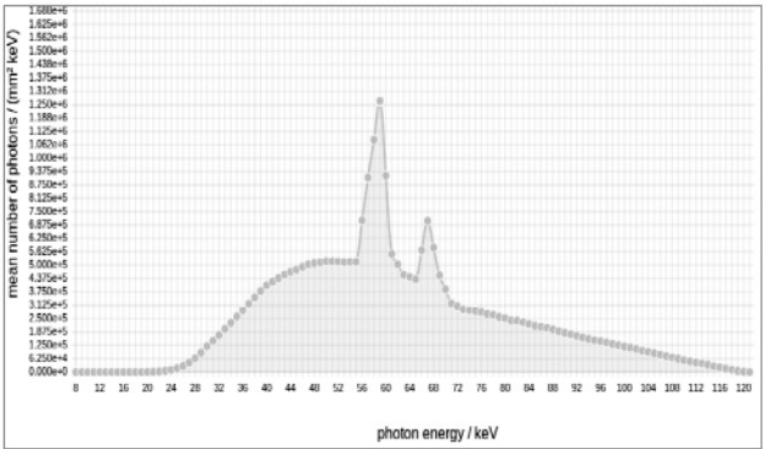

FIGURE 2. spectrum of an X-ray tube in which 120 kVp electrons impact on a tungsten target; resulting bremsstrahlung photons pass through a 3-mm aluminum filter plus a 0.127-mm copper filter (average photon energy is 62 keV).

and 10 MV) with an integrated CBCT. The simulation was divided in two parts: therapeutic and CBCT irradiation.

The first set of simulations incorporates the main components of the beam modifier of a linac. Figure 1 shows the relative positions of the modelled components. In order to reduce computational times, simulations were performed in two steps (Lewis *et al.* 1999).

In the first step concerning therapy, we simulated the beam produced in the linac head: a 6/10 MV electron beam (depending on treatment) was incident on a tungsten target and the emitted bremsstrahlung photons passed through an energy-specific steel-lead flattening filter. Then, a primary collimator consisting of a tungsten block with a hollow center allowed to obtain a conical photon beam whose dose, symmetry and flatness was measured by a couple of monitor chambers. Two spaces of phases (SPh) were created after these elements, at 17 cm from the electron source, one for each beam energy, with high statistics (10^{13} primary electrons) and were considered as the new "primary source of events" for a second simulation. GAMOS allows writing SPh files according to the standard International Atomic Energy Agency (IAEA) format (Capote 2009).

In the second step, we simulated a secondary collimation system, composed of two orthogonal couples of tungsten jaws, which allow to produce square or rectangular beams, followed by a Multi-Leaf Collimation (MLC) system, which involves the presence of 40 pairs of tungsten leafs, 10 cm thick, designed to define beam shape, each with 1 cm width at the isocenter. These therapeutic simulations were run with 10^{10} events.

The geometrical details of LINAC components were taken from the manufacturer's website,[1] from user manuals and from literature (Kądziołka *et al.* 2006; Grevillot *et al.* 2011; Berris *et al.* 2013; Brochu *et al.* 2014). The Elekta kV source is a ventilated X-ray tube and the flat panel for X-ray detection can be placed at three different positions for

[1] www.elekta.com

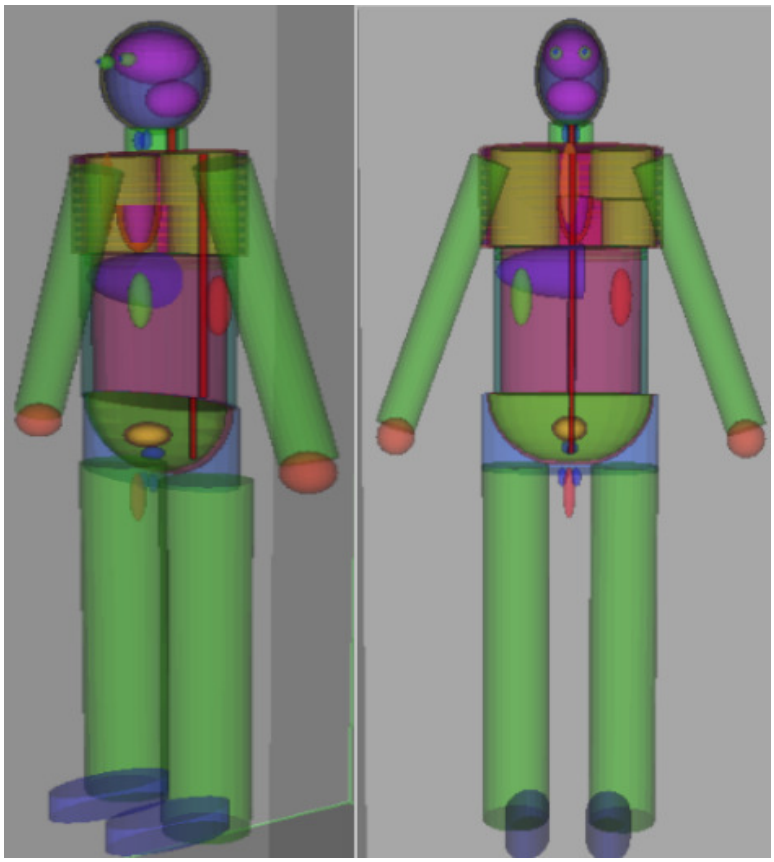

FIGURE 3. Anthropomorphic phantom of an adult male used for our simulation.

small, medium and large field of view (FOV). During the IGRT sessions at Papardo Hospital in Messina the most commonly used protocol employs a tube voltage of 100 kVp for head and neck and 120 kVp for thorax and pelvis; the inherent tube filtration is 0.123 mm of copper and only for thorax and pelvis scans a filter of 3 mm of aluminium is added. The image acquisition and reconstruction software, Elekta XVI, is updated to version 5.0, and the angle of acquisition is 360°.

The X-ray spectrum of CBCT was obtained from a web-based interactive application provided by Siemens, based on an algorithm developed by J. M. Boone (Fewell *et al.* 1981; Boone *et al.* 1997; Boone and Seibert 1997). Through this application it is possible to enter tube specifications, such as maximum voltage, anode and filters composition (Srnivasan *et al.* 2014). The obtained spectra, as in Fig. 2, were input in GAMOS, interpolated in energy and angularly distributed with a 10° opening angle. During our simulations the source was rotated around patient isocenter with 5° angular step; 10^8 events were launched for each of the 72 steps (7.2×10^9 total events).

TABLE 1. Main organs at risk in external beam radiotherapy, where the main simulation parameters, such as geometry, size and material are listed. For spheres, we reported the radius.

Organ	Shape	x (cm)	y (cm)	z (cm)	G4 material	Volume (cm^3)	Density (g/cm^3)
Brain	Ellipsoid	8.5	7.5	6	Brain ICRP	1602.21	1.03
Cerebellum	Ellipsoid	5.6	4	3.5	Brain ICRP	328.40	1.03
Eye	Sphere	1.5	-	-	Water	14.14	1.00
Eye lens	Ellipsoid	0.6	0.3	0.6	Eye lens ICRP	0.45	1.10
Thyroid	Ellipsoid	1	1	2	Tissue soft ICRP	8.38	1.00
Neck marrow	Tube	0.6	0.6	3	Brain ICRP	6.79	1.03
Thoracic marrow	Tube	0.6	0.6	5	Brain ICRP	11.31	1.03
Abdomen marrow	Tube	0.6	0.6	12	Brain ICRP	27.14	1.03
Pelvis marrow	Tube	0.6	0.6	3.25	Brain ICRP	7.35	1.03
Sternum	Ellipsoid	2	0.5	5	Bone cortical ICRP	20.94	1.85
Right Lung	Elliptical tube	7.5	5	9.8	Lung ICRP	2309.07	0.25
Upper lung	Elliptical tube	7	5	5	Lung ICRP	1099.56	0.25
Lower lung	Elliptical tube	6	5	4.8	Lung ICRP	904.78	0.25
Heart	Ellipsoid	4	3.5	4.5	Muscle striated ICRP	153.94	1.05
Blood	Ellipsoid	3	2.5	3.5	Blood ICRP	109.96	1.06
Liver	Ellipsoid	5	4	3	Tissue soft ICRP	251.33	1.00
Kidney	Ellipsoid	2.8	2	3.6	Tissue soft ICRP	84.45	1.00
Prostate	Ellipsoid	2	2	1.5	Tissue soft ICRP	25.13	1.00
Testicle	Ellipsoid	1.1	1	2	Tissue soft ICRP	9.22	1.00
Penis	Ellipsoid	1.4	1	6	Tissue soft ICRP	35.19	1.00
Bladder	Ellipsoid	4	4	2.7	Tissue soft ICRP	62.94	1.00
Urine	Ellipsoid	3.5	3.5	2.3	Water	118.02	1.00
Humeral head	Sphere	1.7	-	-	Bone compact ICRU	20.58	1.85
Femoral head	Sphere	2.5	-	-	Bone compact ICRU	65.45	1.85

To simulate patients, we used an anthropomorphic phantom as in Fig. 3, consisting of five main districts: head, neck, chest, abdomen, pelvis and the four limbs. Shapes and dimensions of the various anatomical districts and organs were taken from literature (Hanavan Jr. 1964; Amato *et al.* 2010, 2016).

We explicitly considered only the most radio-sensitive organs, taken into account by radiation therapists. In Table 1 we listed the organs considered in this study, along with their geometric shape, semi-dimensions along three main axes, material, volume and density. We adopted the ICRP (International Commission on Radiological Protection) and ICRU (International Commission on Radiation Units & Measurements) composition for tissues, taken from the Geant4 materials database.

In order to adapt the phantom to the real patient's anthropometry, we defined three dimensionless parameters, Γ_z, Γ_x and Γ_y, respectively for patient's height, width and thickness. These were determined as the ratio of actual patient size (extrapolated from CT scan) and those of standard anthropomorphic phantom. For organs or regions whose dimension scale with patient's height, organ size was multiplied by the relative scaling factor Γ_i (with $i = x, y, z$). As reported in Table 1, some organs were divided in sub-regions and for each of them GAMOS provided absorbed doses per event. For which concerns

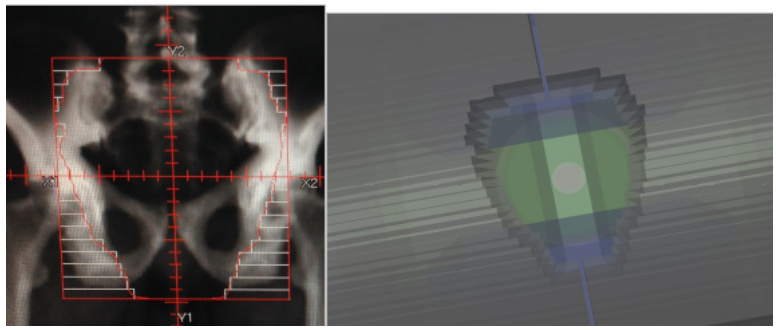

FIGURE 4. left, Philips Pinnacle Beam Eye of View (BEV) of a therapeutic field, representing jaws' margins (red) and leafs (white); right, the same field configuration in three dimensions, obtained by GAMOS.

multi-part organs, average dose was calculated as:

$$D_{TOT} = \frac{m \cdot D_m + M \cdot D_M}{m + M} \tag{1}$$

where D_m is the dose absorbed by mass m, and D_M is the dose absorbed by mass M. We used the GAMOS standard physics list, GmEMPhysics and 0.2 mm of range cut, corresponding to an energy cut of 1 keV, with a calculation time variable from four days for linac source to about a week for CBCT. These choices were based on the outcomes of previous studies, aiming to optimize computational times, without influencing the accuracy of results (Poon and Verhaegen 2005; Faddegon *et al.* 2008; Thiam *et al.* 2008; Geant4 2017). We used GAMOS version 5.0.0, which relies on Geant4 version 4.9.6.p02.

2.2. PDD and profile dose measurements and simulation. In the context of radiation therapy, the most common reference parameter is the percentage depth dose curve (PDD), experimentally measured or computationally calculated in a water phantom, together with transverse profiles of beam both for a SSD=100 cm, a standard field of 10×10 cm^2 at 6 MV and 10 MV. We defined the geometry of a water phantom of $(2x, 2y, 2z)$ size (with $x = y = 88$ mm and $z = 116$ mm) divided in $176 \times 176 \times 116$ voxels placed so that the isocenter falls on the upper surface of the phantom. It was possible to lower the range cut in phantom region only (0.1 mm, corresponding to 0.5 keV), thus improving the sensitivity and accuracy of this set of measurements. The simulation data were compared with experimental measurements, performed using a PTW MP3 water phantom,[2] and a waterproof ionization chamber, movable with a pitch of 2 mm.

2.3. Patients. We adapted our parametric anthropomorphic model to the sizes of six treated patients. Table 2 describes the main patient data, such as ID number, treated district, irradiation technique, number of fields, beam energy, patient's position, isocenter dose as calculated by the Philips Pinnacle[3] TPS, and number of fractions. For each patient, we launched a simulation for each beam angle provided by the treatment plan. Our GAMOS code allowed us to input the positions of jaws and MLC for each projection (Fig. 4), in

[2]http://www.ptw.de/mp3_phantom_tank.html?&cId=5223

TABLE 2. Physical and dosimetric data of patients during treatments with MV linac beams.

Patient IDs	1 - 2		3 - 4		5 - 6	
Anatomical region	Chest		Pelvis		Head and neck	
Technique	3DCRT	3DCRT	3DCRT	3DCRT	IMRT	3DCRT
Number of fields	4	3	4	4	7	2
Angles (weight)	8° (33%)	338° (26.4%)	0° (37%)	0° (29%)	160° (20.49%)	40° (52%)
	192° (33%)	158° (43.6%)	90° (25%)	90° (20%)	109° (11.9%)	220° (48%)
	153° (17%)	57° (30%)	180° (137%)	180° (31%)	58° (8.83%)	
	333° (17%)		270° (25%)	270° (20%)	0° (14.13%)	
					323° (13.07%)	
					250° (10.35%)	
					192° (21.22%)	
Energy (MV)	10	10	10	10	6	6
Patient position	Supine	Supine	Prone	Prone	Supine	Supine
Isocenter total dose (Gy)	68.81	42.21	46.1	45.10	57.1	40.0
Fractions	33	20	25	25	30	20

TABLE 3. Physical and dosimetric data of patients during CBCT scans of IGRT.

Patient IDs	1 - 2	3 - 4	5 - 6
Anatomical region	Chest	Pelvis	Head and neck
Collimation	M20 Fast	M20 Fast	S10
Nominal axial length (cm)	26	26	12.5
Energy (kVp)	120	120	100
Filter	Cu+Al	Cu+Al	Cu
Frame	330	330	183
mAs	528	528	18.3

order to reproduce the shape of the treatment field. During processing, single beam data were summed with proper weights assigned by TPS (see "angles (weight)" in Table 2). For the verification phase of IGRT, we reproduced the protocols implemented in XVI software, whose patient specific details are listed in Table 3. GAMOS results were expressed in Gy/event (absorbed dose normalized by number of events). In order to estimate the dose to patient's organs during IGRT, simulation results were rescaled by the ratio between D_{TPS}(isocenter) and D_{sim}(isocenter).

3. Results and discussion

3.1. Validation of Monte Carlo simulation. Calculations performed for verification of physical and dosimetric properties of the simulated beams were in a full agreement with the measured data in a water phantom.

Figure 5 shows the simulated PDD profiles superimposed on the experimental ones, obtained for a standard 10×10 cm^2 field, for the two energies available on Elekta Synergy medical accelerator (6 and 10 MV). Data were normalized to 1 for the maximum dose located at a depth of about 1.5 cm for 6 MV photon beam and 2.5 cm for 10 MV. Regarding both energy beams, relative per cent differences, calculated as $[100 \cdot (x_i - x_f) - 100]\%$, where x_i is the experimental value and x_f the simulation one, never exceed $\pm 1\%$. In the

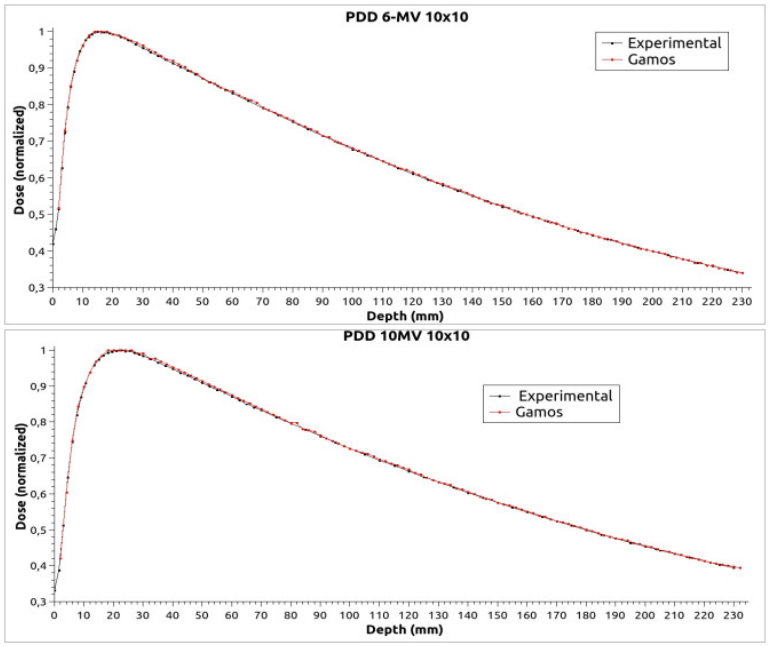

FIGURE 5. Comparison of experimentally measured (black line) and calculated by simulation (red line) PDD curves.

simulated results it is possible to observe small statistical fluctuations of the PDD curve, quite normal for this type of data.

Figure 6 shows the comparison between the simulated in-plane and cross-plane dose profiles (*i*.e., x axis to the top and y axis on the bottom) superimposed to experimental data, for both energies, for a standard field size of 10×10 cm^2. Concerning dose profiles at 6 MV, the percent differences between experimental results and simulation data range from 17% to 1.5% in the penumbra zone, while these differences never exceed 5% in the central region. At 10 MV, the most used in current therapies, percent differences are small and fluctuating between 6% and 0.1% in the entire beam profile, with differences not exceeding 2% in the central region.

3.2. Doses delivered to patients. In Table 4 we report, as a result of our MC simulation, the dose absorbed by various organs and at the isocenter for each patient and each source (MV linac and kV CBCT). Table 4 clearly shows that the highest doses are always limited to the target districts. The doses of two thoracic patients exceeded 50 cGy to left lung, which is the tumor site, associated with a lower dose to heart. Doses of patient no. 1 are slightly higher, because his therapy involved a greater number of fields of larger size. In two pelvic patients, both treated with four fields, bladder (tumor site) received the highest therapeutic doses. The lateral fields (90° and 270°) of patient no. 4 had wider margins, involving an increased dose to prostate. Patient no. 5 had a localized tumor to neck lymph nodes and indeed higher therapeutic doses to thyroid and brain were imparted. Therapeutic dose of

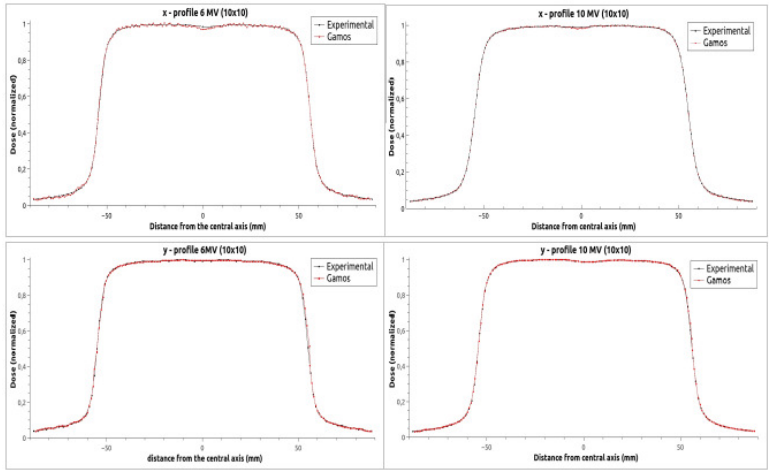

FIGURE 6. In-plane (x) and cross-plane (y) dose profiles for the two available beam energies, for a standard field size of 10 x 10 cm^2; simulated data (red) are superimposed to measured data (black).

patient no. 6 exceeds 50 cGy only for brain (tumor site). Regarding IGRT verification sessions, CBCT doses ranged between almost zero to few mGy for all examined organs, never exceeding 3 cGy in directly scanned districts, except in a few cases.

Effective doses were evaluated, according to the calculation approach and using the tissue-specific weighting factors recommended by the ICRP Publication no. 103 (ICRP 2007) for both diagnostic CBCT and therapeutic irradiations. Results for the six patients are presented in Table 5. As expected, effective doses during therapy are significantly higher than the ones imparted by CBCT. A comparison between the CBCT effective doses evaluated for our patients and the experimental values reported in recent literature (Kan *et al.* 2008) concerning low-dose mode CBCT scans reveal an agreement for the irradiation districts studied.

4. Conclusions

We developed a Monte Carlo simulation in GAMOS, in order to reproduce the operation of a medical linac coupled with a CBCT, and we implemented an anthropomorphic model of patient, in order to quantify doses to the main organs at risk. Our simulations confirmed that the scattered radiation during therapy (MV range) is larger than that diffused by CBCT by one to two orders of magnitude. With these results it should be assumed that the daily use of CBCT to verify the correct positioning of the patient during radiotherapy sessions, on one hand allows to optimize the dose delivery and on the other one it does not cause excessive dose absorption to the organs at risk.

TABLE 4. Doses (mGy) absorbed by various organs obtained through GAMOS MC simulation, from linac (MV energy range) and CBCT (kV energy range), concerning a single irradiation.

Patient ID	1		2		3		4		5		6	
Source	Linac	CBCT	Linac	CBCT	Linac	CBCT	Linac	CBCT	Linac	CBCT	Linac	CBCT
Energy	10 MV	120 kV	10 MV	120 kV	10 MV	120 kV	10 MV	120 kV	6 MV	120 kV	6 MV	120 kV
Brain	2.18	0.47	1.18	0.23	4.24	0.00	1.95	0.00	404.89	0.38	639.49	46.15
Right eye	0.44	0.05	0.04	0.04	1.12	0.00	0.29	0.00	13.91	0.20	3.52	0.17
Left eye	0.41	0.05	0.06	0.03	1.03	0.00	0.13	0.00	13.31	0.20	2.59	0.17
Right eye lens	3.41	0.03	0.00	0.11	0.00	0.00	0.31	0.00	14.56	0.05	7.48	0.11
Left eye lens	3.30	0.03	0.00	0.11	0.00	0.00	0.30	0.00	13.82	0.04	7.81	0.11
Right thyroid	108.29	9.23	8.85	1.24	4.33	0.06	40.22	0.03	530.70	0.35	7.86	0.16
Left thyroid	112.13	8.95	9.16	1.54	4.23	0.05	39.22	0.04	531.20	0.36	7.99	0.17
Sternum	224.17	78.27	57.22	4.97	0.15	0.01	1.03	0.01	67.27	0.41	12.69	0.49
Rt humeral head	1.03	3.32	0.57	0.93	0.90	0.00	0.43	0.00	50.37	0.30	4.49	0.29
Lt humeral head	1.08	3.22	0.62	0.98	0.96	0.00	0.49	0.00	48.17	0.29	6.56	0.33
Right lung	30.27	6.99	126.27	3.96	4.86	0.01	4.16	0.08	7.14	0.02	1.54	0.18
Left lung	852.27	6.26	641.27	4.86	5.44	0.10	4.13	0.07	6.53	0.02	1.57	0.18
Heart	248.48	13.27	176.48	0.52	0.75	0.02	0.91	0.01	17.56	0.03	3.54	1.02
Marrow	94.14	9.21	48.14	3.48	460.47	6.25	251.87	4.15	40.38	0.22	17.47	1.10
Liver	11.74	8.14	7.29	4.01	3.42	0.21	6.03	0.05	5.19	0.01	0.95	0.11
Right kidney	2.80	1.06	2.59	0.02	8.61	0.51	18.38	0.14	1.64	0.00	2.18	0.90
Left kidney	4.72	1.91	2.30	0.42	8.58	0.52	16.94	0.13	1.89	0.00	2.34	0.91
Prostate	0.51	0.02	0.69	0.51	49.18	10.10	1628.36	14.25	0.45	0.03	0.91	0.12
Bladder	0.18	0.03	0.19	0.14	1798.2	10.07	1721.8	12.08	0.38	0.01	0.72	0.14
Rt femoral head	0.12	0.02	0.71	0.21	188.23	15.46	114.90	21.73	0.36	0.00	0.28	0.03
Lt femoral head	0.49	0.02	0.40	0.03	181.79	16.05	138.47	21.46	0.36	0.00	0.73	0.03
Right testicle	0.91	0.01	0.91	0.04	112.93	1.12	43.27	1.63	1.36	0.02	0.87	0.18
Left testicle	0.94	0.01	1.02	0.02	112.20	1.02	42.95	1.66	1.43	0.02	0.87	0.17
Isocenter	2079.1	162.6	2029.0	131.7	1844.0	156.1	1804.0	149.1	1903.3	149.4	2000	215.19

TABLE 5. Effective doses evaluated for the six patients during CBCT and therapeutic irradiations.

Patient ID	Anatomical region	H_{linac} (mSv)	H_{CBCT} (mSv)
1	Chest	31.9	5.5
2	Chest	29.2	2.2
3	Pelvis	38.6	1.4
4	Pelvis	37.8	1.2
5	Head and neck	33.6	0.7
6	Head and neck	9.6	0.7

References

Agostinelli, S. *et al.* (2003). "GEANT4 – A simulation toolkit". *Nuclear Instruments and Methods in Physics Research, Section A: Accelerators, Spectrometers, Detectors and Associated Equipment* **506**(3), 250–303. DOI: 10.1016/S0168-9002(03)01368-8.

Amato, E., Asero, G., Leotta, S., Auditore, L., Salamone, I., Mannino, G., Privitera, S., and Gueli, A. (2016). "Influence of the X-ray beam quality on the dose increment in CT with iodinated contrast medium". *Journal of X-Ray Science and Technology* **24**(2), 267–278. DOI: 10.3233/XST-160551.

Amato, E., Italiano, A., and Baldari, S. (2013a). "Absorbed fractions for alpha particles in ellipsoidal volumes". *Physics in Medicine and Biology* **58**(16), 5449–5459. DOI: 10.1088/0031-9155/58/16/5449.

Amato, E., Italiano, A., Minutoli, F., and Baldari, S. (2013b). "Use of the GEANT4 Monte Carlo to determine three-dimensional dose factors for radionuclide dosimetry". *Nuclear Instruments and Methods in Physics Research, Section A: Accelerators, Spectrometers, Detectors and Associated Equipment* **708**, 15–18. DOI: 10.1016/j.nima.2013.01.014.

Amato, E., Lizio, D., Ruggeri, R. M., Raniolo, M., Campennì, A., and Baldari, S. (2011). "An analytical model for improving absorbed dose calculation accuracy in non spherical autonomous functioning thyroid nodule". *Quarterly Journal of Nuclear Medicine and Molecular Imaging* **55**(5), 560–566. URL: https://www.minervamedica.it/it/riviste/nuclear-med-molecular-imaging/articolo.php?cod=R39Y2011N05A0560.

Amato, E., Lizio, D., Settineri, N., Di Pasquale, A., Salamone, I., and Pandolfo, I. (2010). "A method to evaluate the dose increase in CT with iodinated contrast medium". *Medical Physics* **37**(8), 4249–4256. DOI: 10.1118/1.3460797.

Amato, E., Minutoli, F., Pacilio, M., Campennì, A., and Baldari, S. (2012). "An analytical method for computing voxel S values for electrons and photons". *Medical Physics* **39**(11), 6808–6817. DOI: 10.1118/1.4757912.

Arce, P., Lagares, J. I., Harkness, L., Desorgher, L., De Lorenzo, G., Abreu, Y., and Wang, Z. (2012). "GAMOS: An easy and flexible way to use GEANT4". *IEEE Nuclear Science Symposium Conference Record*, 2230–2237. DOI: 10.1109/NSSMIC.2011.6154455.

Berris, T., Mazonakis, M., Stratakis, J., Tzedakis, A., Fasoulaki, A., and Damilakis, J. (2013). "Calculation of organ doses from breast cancer radiotherapy: a Monte Carlo study". *Journal of Applied Clinical Medical Physics* **14**(1), 133–146. DOI: 10.1120/jacmp.v14i1.4029.

Boone, J. M., Fewell, T. R., and Jennings, R. J. (1997). "Molybdenum, rhodium, and tungsten anode spectral models using interpolating polynomials with application to mammography". *Medical Physics* **24**(12), 1863–1874. DOI: 10.1118/1.598100.

Boone, J. M. and Seibert, J. A. (1997). "An accurate method for computer-generating tungsten anode x-ray spectra from 30 to 140 kV". *Medical Physics* **24**(11), 1661–1670. DOI: 10.1118/1.597953.

Brochu, F. M., Burnet, N. G., Jena, R., Plaistow, R., Parker, M. A., and Thomas, S. J. (2014). "Geant4 simulation of the Elekta XVI kV CBCT unit for accurate description of potential late toxicity effects of image-guided radiotherapy". *Physics in Medicine and Biology* **59**(24), 7601–7608. DOI: 10.1088/0031-9155/59/24/7601.

Capote, R. (2009). *Phase-space database for external beam radiotherapy*. IAEA NAPC Nuclear Data Section – IAEA NAHU Dosimetry and Medical Radiation Physics Section. URL: http://www-nds.iaea.org/phsp/phsp.htmlx.

Faddegon, B. A., Asai, M., Perl, J., Ross, C., Sempau, J., Tinslay, J., and Salvat, F. (2008). "Benchmarking of Monte Carlo simulation of bremsstrahlung from thick targets at radiotherapy energies". *Medical Physics* **35**(10), 4308–4317. DOI: 10.1118/1.2975150.

Fewell, T. R., Shuping, R. E., Hawkins, K. R., and United States. Bureau and of Radiological Health. Division of Electronic Products (1981). *Handbook of Computed Tomography X-ray Spectra*. (Radiological Health). U.S. Government Printing Office.

Geant4 (2017). *Physics Reference Manual*. URL: http://geant4.web.cern.ch/geant4/UserDocumentation/UsersGuides/PhysicsReferenceManual/html/index.html.

Grevillot, L., Frisson, T., Maneval, D., Zahra, N., Badel, J.-N., and Sarrut, D. (2011). "Simulation of a 6 MV Elekta Precise Linac photon beam using GATE/GEANT4". *Physics in Medicine and Biology* **56**(4), 903–918. DOI: 10.1088/0031-9155/56/4/002.

Hanavan Jr., E. P. (1964). *A mathematical model of the human body*. Tech. rep. AMRL-TR-64-102. Wright-Patterson Air Force Base, Ohio : Aerospace Medical Research Laboratories.

ICRP (2007). "The 2007 Recommendations of the International Commission on Radiological Protection. ICRP Publication 103". *Annals of the ICRP* **37**(2-4). URL: http://www.icrp.org/publication.asp?id=ICRP%20Publication%20103.

Kądziołka, E., Kisielewska-Birycka, M., Surowiak, T., Barszczewski, J., and Kukołowicz, P. F. (2006). "Information about the first Elekta Precise® accelerator installed in Poland". *Reports of Practical Oncology and Radiotherapy* **11**(3), 147–155. URL: https://www.sciencedirect.com/science/article/pii/S1507136706710604.

Kan, M. W., Leung, L. H., Wong, W., and Lam, N. (2008). "Radiation dose from cone beam computed tomography for image-guided radiation therapy". *International Journal of Radiation Oncology Biology Physics* **70**(1), 272–279. DOI: 10.1016/j.ijrobp.2007.08.062.

Lewis, R. D., Ryde, S. J., Hancock, D. A., and Evans, C. J. (1999). "An MCNP-based model of a linear accelerator x-ray beam". *Physics in Medicine and Biology* **44**(5), 1219–1230. DOI: 10.1088/0031-9155/44/5/010.

Moore, C. J., Amer, A., Marchant, T., Sykes, J. R., Davies, J., Stratford, J., McCarthy, C., MacBain, C., Henry, A., Price, P., and Williams, P. C. (2006). "Developments in and experience of kilovoltage X-ray cone beam image-guided radiotherapy". *British Journal of Radiology* **79** (Special issue 1), S66–S78. DOI: 10.1259/bjr/68255935.

Poon, E. and Verhaegen, F. (2005). "Accuracy of the photon and electron physics in GEANT4 for radiotherapy applications". *Medical Physics* **32**(6), 1696–1711. DOI: 10.1118/1.1895796.

Srnivasan, K., Mohammadi, M., and Shepherd, J. (2014). "Applications of linac-mounted kilovoltage Cone-beam Computed Tomography in modern radiation therapy: A review". *Polish Journal of Radiology* **79**, 181–193. URL: http://archiwum.polradiol.com/archives/issue/idIssue/835187.html.

Thiam, C. O., Breton, V., Donnarieix, D., Habib, B., and Maigne, L. (2008). "Validation of a dose deposited by low-energy photons using GATE/GEANT4". *Physics in Medicine and Biology* **53**(11), 3039–3055. DOI: 10.1088/0031-9155/53/11/019.

---

[a] Radiosurgery Center
Agropoli, Italy

[b] Università degli Studi di Messina
Dipartimento di Scienze Biomediche, Odontoiatriche e delle Immagini Morfologiche e Funzionali
Messina, Italy

[c] Istituto Nazionale di Fisica Nucleare
Sezione di Catania, Catania, Italy

[d] Azienda Ospedaliera Papardo
Messina, Italy

[e] Azienda Ospedaliera Universitaria Policlinico "G. Martino"
Messina, Italy

[*] To whom correspondence should be addressed | email: eamato@unime.it

Communicated 30 November 2017; manuscript received 4 December 2017; published online 23 February 2018